CO oxidation on $Au/TiO_x/Mo\{112\}$: Structure characterization and catalytic activity studied using *ab initio* calculations

Zhi-Pan Liu*

Shanghai Key Laboratory of Molecular Catalysis and Innovative Materials, Department of Chemistry, Fudan University, Shanghai, 200433, People's Republic of China

(Received 14 April 2006; published 30 June 2006)

Low-temperature CO oxidation over Au/oxides attracts alot of interest for its industrial and scientific importance. To date, it remains controversial where it occurs. Recently, Chen and Goodman suggested the reaction can occur on Au itself from their experiment of CO oxidation over $Au/TiO_x/Mo\{112\}$. Here, using *ab initio* thermodynamic calculations we determined the chemical stoichiometry of the TiO_x film as TiO_3 and resolved the geometrical structure of the TiO_3 and the subsequent Au films. The segregation is revealed to be favored upon Au deposition/annealing on the $TiO_3/Mo\{112\}$. The interface between Au and TiO_3 that is supported on Mo{112} is identified as the only reaction site. The *superior* reactivity of a "two-layer Au film" is then rationalized.

DOI: 10.1103/PhysRevB.73.233410 PACS number(s): 68.35.−p, 68.43.Bc, 82.65.+r

Since the discovery of the catalytic ability of Au,[1] considerable efforts have been devoted to reveal the catalytic mechanism.[2–14] Among the most intriguing features, one must rank the so-called two-layer Au reactivity, first reported by Valden *et al.*[2] They discovered that in CO oxidation on $Au/TiO_2\{110\}$ the *two-layer Au* particles are the most active, not the one- or multilayer Au. Experimentally, the high activity of Au particles at particular sizes was attributed to several possible reasons, such as the quantum size effect, the activity of low-coordinated Au, and the synergetic effect occurring at the interface.[1–7] Using density functional theory (DFT) calculations, CO oxidation over Au/TiO_2 were studied and the Au/oxide *interface* was found to be essential for O_2 activation.[8–13] More recently, Chen and Goodman conducted a new experiment for CO oxidation over Au film on an elegantly prepared $TiO_x/Mo\{112\}$.[8,9] Their results imply that CO oxidation can occur on Au *without* involving an Au/oxide interface.

The new experiment of Chen and Goodman is briefly summarized here (more details can be found in Refs. 8 and 9). Under ultrahigh-vacuum conditions, a TiO_x thin film on Mo{112} can be synthesized by either annealing a TiO_x/SiO_x mixed layer or repeatedly depositing/annealing TiO_x on Mo{112} to 1400 K. The prepared TiO_x film exhibits a $p(8\times2)$ low-energy electron diffraction (LEED) pattern and the oxidation state of Ti is suggested to be Ti^{3+}. By depositing Au onto the $TiO_x/Mo\{112\}$ followed by annealing at 900 K, a structure with a clear $p(1\times1)$ LEED pattern is obtained. This LEED pattern is attributed to 1 ML Au on $TiO_x/Mo\{112\}$ based on Auger signals. With the increase of Au coverage, a new LEED pattern, $p(1\times3)$, is observed, which is assigned to a two-layer Au film. CO oxidation was then performed on the (1×1) phase and the (1×3) phase. It was found that CO oxidation on the (1×3) phase is significantly faster than on the (1×1) phase and also 45 times faster than on the Au/TiO_2.[4,8]

For its extraordinary catalytic ability, the $Au/TiO_x/Mo\{112\}$ surface itself warrant further detailed studies. On the other hand, the experiment seems to be contradictory to the results of previous DFT studies[10–13] and some experimental views,[1–3,14] in which the Au/oxide interface is suggested to be reaction sites. Although other possibilities may contribute to reconcile the inconsistency,[8] so far none of the speculations can be confirmed because the atomic structures of the TiO_x film and the Au films are not resolved.

Although *ab initio* theoretical calculation would be an ideal approach to validate the above speculations, three major difficulties have to first be considered in hunting for the structure of $TiO_x/Mo\{112\}$. (i) The system is a large metallic system with a simulation cell of at least $p(8\times2)$ Mo{112} according to experiment, which typically contains more than 60 metal atoms; (ii) the chemical stoichiometry of TiO_x (the value of x) is entirely unknown; (iii) the annealing temperature and the O_2 partial pressure are crucial. The recently-developed *ab initio* thermodynamics method[15,16] on the basis of parallel density functional theory calculation, such as that implemented in the SIESTA package used here, provides a good chance to solve this type of problem.[11] To further speed up calculations, here the Kohn-Sham equation is solved by an iterative parallel diagonalization method that utilizes the SCALAPACK[17] subroutine pdsygvx with a two-dimensional block cyclically distributed matrix. Because a Γ-point calculation is much faster in parallel SIESTA, the Mo{112} surface of $TiO_x/Mo\{112\}$ is routinely modeled by a four layer (8×2) unit cell $(21.87\times8.93$ Å) with its top two-layers fully relaxed, and the final energy is obtained using the double-sized cell, i.e., (8×4) $(21.87\times17.86$ Å). The other details of calculation setup in SIESTA are described in Ref. 18.

As the growth of the TiO_x film on Mo{112} is self-limited,[9] the obtained TiO_x film should be the most favored structure thermodynamically. At the thermodynamic equilibrium the chemical potential of elements, μ(Ti), μ(O), and μ(Mo), are the same everywhere in the system. Accordingly, we have used the following procedure to determine the structure of TiO_x on Mo{112} at the (T,p). Hereafter T and p are 1400 K and $p_{o2}=1.3\times10^{-11}$ atm $(1\times10^{-8}$ torr), respectively.[8]

(i) μ(O) is pinned by that of the gas phase O_2. As $\mu(O)=1/2\mu(O_2)$, it can be first calculated. With the thermodynamic equations and the tabulated thermodynamic data (the

derivation procedure was described in our previous paper, Ref. 13), $\mu(O)$ at the (T,p) is calculated to be 3.13 eV lower than that of O in O_2 at 0 K:

$$\mu(O) = -3.13 + 1/2E_{tot}(O_2), \quad (1)$$

where $E_{tot}(O_2)$ is the DFT total energy of O_2 at 0 K with the zero-point energy included.

(ii) To know the possible form of Ti oxide bulk, TiO_2 or Ti_2O_3, which may coexist with the TiO_x film, we can calculate the Gibbs free energy change ΔG of $TiO_2(bulk) \rightarrow 1/2\ Ti_2O_3(bulk) + 1/4\ O_2(gas)$ at the (T,p).

$$\Delta G \approx 1/2E_{tot}(Ti_2O_3) + 1/2\mu(O) - E_{tot}(TiO_2). \quad (2)$$

For the solid states, the DFT-calculated total energy, E_{tot} (strictly speaking, the Helmholtz free energy at 0 K *and* neglecting zero-point vibrations), is used to represent the corresponding Gibbs free energy at finite T and p. This approximation is justified because the corresponding corrections that enter into $G(T,p)$ are small (see, e.g., Refs. 15 and 16). From Eqs. (1) and (2), ΔG is calculated to be +0.38 eV (endothermic). Therefore, TiO_2 is the most stable form of Ti oxide bulk at the (T,p).

(iii) Next, we guess for a TiO_x structure on Mo{112} and optimize its structure to get the total energy, $E_{tot}(TiO_x/Mo\{112\})$. The stability of such a TiO_x film on Mo{112} can be measured from the ΔG_f of the reaction, $Mo\{112\} + nTiO_2(bulk) + n(x-2)/2\ O_2(g) \rightarrow nTiO_x/Mo\{112\}$:

$$\Delta G_f = 1/n[E_{tot}(nTiO_x/Mo\{112\}) - E_{tot}(Mo\{112\}) - nE_{tot}(TiO_2) - n(x-2)\mu(O)], \quad (3)$$

where n is the number of TiO_x per Mo{112} unit cell modeled. Combine Eqs. (1) and (3), and ΔG_f can be calculated from DFT. According to Eq. (3), a TiO_x film is existing only when $\Delta G_f < 0$ and the lowest ΔG_f corresponds to the most stable TiO_x film. It should be mentioned that for promising structures (low ΔG_f) additional simulation with a Nose thermostat molecular dynamics (MD) (1000 K, 1 fs/step, 500–1000 steps) is performed to avoid trapping in local minima. Generally, we found a MD simulation is rather essential for complex structures.

Using the above procedure we investigated a large number of TiO_x films, where the x value is varied from 1 to 4 and the convergence θ_{Ti} ($Ti:Mo^{top\ layer}$) is varied from 0.44 (7/16) to 3 ML. Table I listed the ΔG_f of the most stable configurations at selected x and θ_{Ti} values. A structure with the highest stability is discovered, that is, 0.44 ML TiO_3 on Mo{112}. As TiO_3 contains even more oxygen than TiO_2 bulk, it is indicated that surface Mo atoms do provide coordinations to the excess O atoms since Ti does not exhibit oxidation states more than +4 in nature. The presence of an O-Mo bond also explains the repulsive interaction between TiO_x at high θ_{Ti} as implied from Table I due to the so-called *bonding competition effect*.[16]

Three TiO_x films in Table I that represent the most stable configurations of $x > 2$ might be of most interest. The structures of $TiO_{2.5}$, TiO_3 and TiO_4, are highlighted in Figs. 1(a)–1(c), respectively. The $TiO_{2.5}$ [$Ti_{14}O_{35}$ per $p(8\times2)$ unit cell] film is built from TiO_4 tetrahedrons that forms a ring-by-ring structure directly above one of every two troughs of Mo{112}. Each ring contains four TiO_4 tetrahedrons and every eight Mo atoms accommodate seven TiO_4 tetrahedrons due to the surface stress along the x direction. The TiO_3 film is composed of separated [-O-TiO_2-O-] rows, each row occupying one of every two trenches of Mo{112}. It has a $p(8\times2)$ periodicity with every 8 Mo surface atoms holding 7 TiO_4 units. The TiO_4 film covers the whole Mo surface with separated TiO_4 units that arrange in the $c(2\times2)$ periodicity. Among the three structures, only the most stable TiO_3 film appears to be consistent with the LEED pattern $[p(8\times2)]$[8] and the STM observation that shows rows with alternated protrusion and depression.[9] As further proof, the vibrational frequencies at the Γ point of the three films have also been calculated by the finite-displacement technique and the modes with the dynamic dipole moment normal to surface were selected. In line with the energetics, we found that the TiO_3 film exhibits a Ti-O-Ti mode 82.9 meV, very close to the experimental value 84 meV,[9] while the $TiO_{2.5}$ and TiO_4 are at 97.9 meV (Ti-O-Ti mode) and 81.1 (Ti-O-Mo mode) meV, respectively.

TABLE I. Calculated energetics (ΔG_f, unit: eV) and periodicity of selected TiO_x films on Mo{112} at 1400 K, $p_{O2} = 1\times10^{-8}$ torr.

x (O:Ti)	θ_{Ti}	ΔG_f	Periodicity
1	1	0.74	$p(1\times1)$
1.5	2	0.38	$p(1\times1)$
1.5	1	0.18	$p(1\times2)$
1.94	1	−0.23	$p(8\times2)$
2	0.5	−0.99	$p(1\times2)$
2	1	−0.29	$p(1\times2)$
2.5	1	−0.71	$p(8\times2)$
2.5	2	−0.06	$p(1\times1)$
2.5	**0.88**	**−0.80**	**p(8×2)**
3	0.5	−1.32	$p(1\times2)$
3	**0.44**	**−1.66**	**p(8×2)**
3	1	−0.28	$p(1\times1)$
4	**0.5**	**−0.17**	**c(2×2)**

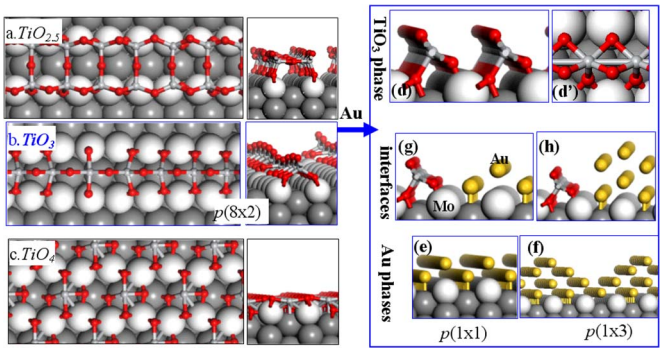

FIG. 1. (Color online) Top and side view of the (a) $TiO_{2.5}$, (b) TiO_3, (c) TiO_4 films (see Table I). The right-hand frames collect the structures after Au deposition/annealing on (b), namely (d,d′) the TiO_3 phase, (e,f) the Au phases, and (g, h) the interfaces.

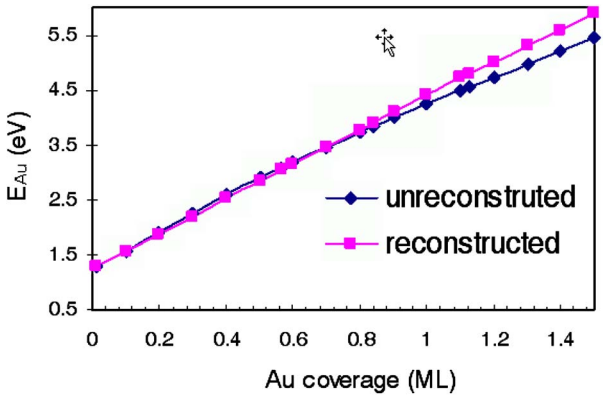

FIG. 2. (Color online) Plot of E_{Au} (eV) against Au coverage (ML), showing the energy gain of Au growth on the unreconstructed [Fig. 1(b)] and reconstructed [Fig. 1(d)] TiO_3/Mo{112}.

Having characterized the TiO_x film, the next step is to understand how Au grows on it. Immediately, we realized that Au directly growing on top of the TiO_3 film can achieve neither a $p(1\times1)$ nor a $p(1\times3)$ structure. Thus, we speculated that the TiO_3 film may undergo reconstruction. To test this, we took one Au atom as a probe and optimized this Au adatom on a clean Mo{112} and on the TiO_3/Mo{112}. It was found that the Au atom adsorbs most strongly on the clean Mo{112} [E_{ad}(Au)=4.03 eV, this is much stronger than the Au cohesive energy, 3.2 eV from our DFT], while its adsorption energies on the TiO_3/Mo{112} are much smaller, i.e., 3.39 eV in the unoccupied trench of TiO_3/Mo{112} and 1.25 eV on the exposed O of the TiO_3 film. This implies that a surface reconstruction to expose clean Mo{112} might be favored upon Au deposition.

Along this line, we have proposed a picture for Au growth on TiO_3/Mo{112}. With Au deposition, the original TiO_3 film may start to condense into a close-packed TiO_3 film, which can gradually expose clean Mo{112} surface sites (a complete condensation would provide $1-7/16=0.56$ ML free surface sites). This process is endothermic. This close-packed TiO_3 film has a (1×1) periodicity, as depicted in Fig. 1(d), and the Ti is fivefold, very similar to the surface Ti in TiO_2{110}. At the mean time, Au can grow on the open Mo{112} epitaxially. This latter process is exothermic. In order to find out at what Au coverage the reconstruction could happen, we calculated the overall energy profile for Au adsorption on the unreconstructed and the reconstructed surfaces, as shown in Fig. 2, where the total energy gain (E_{Au}) is plotted against Au coverage. Generally, the E_{Au} is calculated using:

$$E_{Au} = -\theta_{Ti}\Delta G_f - \theta_{Ti}^{rec}\Delta G_f^{rec} + \int E_{ad}^{diff} d\theta_{Au}$$

$$\approx -\theta_{Ti}\Delta G_f - \theta_{Ti}^{rec}\Delta G_f^{rec} + \sum E_{ad}^{quasi\text{-}diff}\Delta\theta_{Au}, \quad (4)$$

where ΔG_f and ΔG_f^{rec} are the same as that in Table I except the temperature is now 900 K at annealing for the two TiO_3 phases. At 900 K, ΔG_f is calculated to be −2.85 eV for the unreconstructed TiO_3 (note: −1.66 eV in Table I is at 1400 K) and ΔG_f^{rec} is −1.32 eV for the reconstructed TiO_3. E_{ad}^{diff} is the differential adsorption energy of Au. Because E_{ad}^{diff} is not easily obtainable in periodic DFT calculations, we, instead, adopted its computable approximation, namely quasidifferential adsorption energy $E_{ad}^{quasi\text{-}diff}=E_{ad}^{\Delta\theta}/\Delta\theta_{Au}$ where $E_{ad}^{\Delta\theta}$ is the integral adsorption energy of the nth $\Delta\theta_{Au}$ ML Au atoms on the $(n$-1)th $\Delta\theta_{Au}$ covered surface ($n=1,2,\ldots$).[16] Obviously, when $\Delta\theta_{Au}$ goes to infinitely small, $E_{ad}^{quasi\text{-}diff}=E_{ad}^{diff}$. It should be mentioned that in calculating E_{Au} for Au adsorption on the reconstructed surface (Fig. 2), the variation of local Au coverages is allowed. In particular, we found that below 1.13 ML Au coverage, (1×1) 2 ML Au on Mo{112} are always preferred with the surface consisting of Au domains, unconstructed TiO_3 domains, and condensed TiO_3 domains.

Figure 2 shows clearly a crossing point at Au coverage around 0.7 ML. Above this coverage, the reconstructed phase starts to win over the unreconstructed one. Furthermore, the (1×1) Au/TiO_x/Mo phase observed corresponds to ~1.31 (0.56×2) ML of Au [in fact from 0.7 ML (1×1) pattern can appear if the kinetic is not a problem]; the (1×3) phase corresponds to ~1.69 $(=0.56\times3)$ ML. The structures and the resulting interfaces are shown in Figs. 1(e)–1(h). Our results indicate that the experimentally observed LEED pattern after the Au deposition is originated from a Au/Mo{112} rather than an Au/TiO_x/Mo{112} and the "one- and two-layer Au phases"[8] have in fact two and three layers of Au, respectively. It should be noticed that the (1×1) Au phase here consists of 2 ML Au domains and condensed TiO_3 domains with no Mo exposed, which is different from a freshly prepared 1 ML Au/Mo{112} that also exhibits a (1×1) LEED pattern at RT.[8] The latter one loses (1×1) pattern after annealing to 900 K at $p_{O2}=10^{-8}$ torr,[8] which can be explained as the exposed Mo (second layer) on the 1 ML Au/Mo{112} can dissociate O_2 and the O atoms compete with Au for surface Mo sites.

By introducing CO and O_2 onto the Au/TiO_3/Mo{112}, we further investigated the catalytic activity for CO oxidation. The O_2 adsorption on the individual phases was first studied. It was found that O_2 only weakly adsorbs on the segregated phases, 0.34 eV on the TiO_3 phase, and 0.13 and 0.16 eV on the two Au phases. Such low adsorption ability of O_2 is unlikely to account for the room temperature CO oxidation activity. Thus, we turned to the interfaces [Figs. 1(g) and 1(h)]. Our simulation cell used for the interfaces is (4×4) $(10.9\times17.8$ Å), which is evenly divided into a TiO_3 region and an Au region, each occupying a (4×2) area. We found O_2 adsorption is much enhanced at the interfaces: 1.78 and 1.66 eV for the (1×1) and (1×3) interfaces, respectively. In both cases, O_2 adsorbs at the top of a five-fold Ti at the interface with additional bonding with the nearby Au.

Then, the CO+O_2 reaction at the interfaces was calculated and the transition states were located using the constrained minimization technique.[10–12] It was found that the CO can react with O_2 easily at both interfaces and the reaction barriers in the processes are all below 0.1 eV. The reaction pathway of the CO+O_2 reaction is similar to that identified previously[11] and thus is only briefly described here. At the initial state, CO adsorbs on edge Au atoms at the inter-

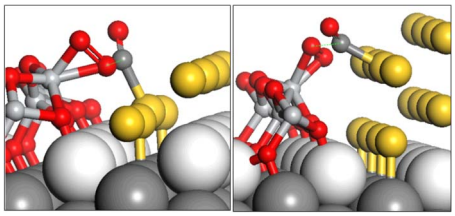

FIG. 3. (Color online) $CO+O_2$ transition states at the (1×1) interface (left) and the (1×3) interface (right).

faces: $E_{ad}(CO)$ is 0.57, 0.80 eV for the (1×1) and (1×3) phases, respectively. The CO can react with O_2 through a bimolecular mechanism. The located transition states (TS) at the two interfaces are illustrated in Fig. 3. At the (1×1) interface, the CO_2 and O are directly produced after the TS. In contrast, at the (1×3) interface a metastable COO_2 complex is formed right after the TS, which then decomposes into CO_2 and an adsorbed O atom. In the final step, another coming CO reacts off the adsorbed O atom to form a second CO_2.

Once we combine thermodynamics and DFT calculations, we found that the Au/TiO_3 interfaces are the only active site for CO oxidation, agreeing with our earlier DFT study for CO oxidation on the Au/Ti{110}.[11] As the reaction barriers calculated are very low, it is expected that the other factors, such as the pre-exponential factor, the concentration of interface sites, and the coverage of O_2 and CO at the interfaces, should play the determining role in the reaction rate. Considering that the reaction rate is measured at room temperatures experimentally, the lower adsorption energy of CO at the (1×1) interface (0.57 eV) compared to that at the (1×3) (0.80 eV) could be the key as to why the (1×3) phase is much more active. From a simple adsorption-desorption kinetics, it can be estimated that the CO concentration at the (1×3) interface is three orders of magnitude larger than (1×1) at 300 K.

To recap, this work represents the first attempt to determine the reaction site of CO oxidation on a specific new $Au/TiO_x/Mo\{112\}$ model catalyst with close relevance to the important field of Au nanocatalysis. Our major finding is that segregation is favored at the stage of Au deposition/annealing on the identified $TiO_3/Mo\{112\}$. We show that both Au and TiO_3 bond very strongly on Mo{112}, and the interfaces between the supported Au and the supported TiO_3 are the active sites for CO oxidation. Through this surprising architecture, namely, *Au plus oxide on a metal*, both the high stability (the Au sintering is unlikely as the Au-Mo bonding is much stronger than Au-Au) and the high reactivity can be achieved. The extraordinary activity of the "two-layer Au phase" in $Au/TiO_x/Mo\{112\}$ is also rationalized.

This work was supported by National Natural Science Foundation of China (Grant No. 20573023, 20433020) and the National Science Foundation of Shanghai Science and Technology Committee (05DZ22313). We are grateful to the Shanghai Supercomputing Center for their allocation of computer time.

*Email address: zpliu@fudan.edu.cn

[1] M. Haruta, Catal. Today **36**, 153 (1997).
[2] D. A. Outka and R. J. Madix, Surf. Sci. **179**, 351 (1987).
[3] R. Meyer, C. Lemire, K. Sh. Shaikhutdinov, and H. J. Freund, Gold Bull. **37**, 72 (2004).
[4] M. Valden, X. Lai, and D. W. Goodman, Science **281**, 1637 (1998).
[5] J. D. Grunwaldt, C. Kiener, C. Wogerbauer, and A. Baiker, J. Catal. **186**, 458 (1999).
[6] V. A. Bondzie, S. C. Parker, and C. T. Campbell, J. Vac. Sci. Technol. A **17**, 1717 (1999).
[7] Q. Fu, H. Saltsburg, and M. Flytzani-Stephanopoulos, Science **301**, 935 (2003).
[8] M. S. Chen and D. W. Goodman, Science **306**, 252 (2004); C. T. Campell, *ibid.* **306**, 234 (2004).
[9] M. S. Chen, W. T. Wallace, D. Kumar, Z. Yan, K. K. Gath, Y. Cai, Y. Kuroda, and D. W. Goodman, Surf. Sci. **581**, L115 (2005).
[10] Z.-P. Liu, P. Hu, and A. Alavi, J. Am. Chem. Soc. **124**, 7499 (2002).
[11] Z.-P. Liu, X.-Q. Gong, J. Kohanoff, C. Sanchez, and P. Hu, Phys. Rev. Lett. **91**, 266102 (2003).
[12] Z.-P. Liu, S. J. Jenkins, and D. A. King, Phys. Rev. Lett. **93**, 156102 (2004).
[13] L. M. Molina and B. Hammer, Phys. Rev. Lett. **90**, 206102 (2003).
[14] J. D. Stiehl, T. S. Kim, S. M. McClure, and C. B. Mullins, J. Am. Chem. Soc. **124**, 7499 (2004).
[15] K. Reuter and M. Scheffler, Phys. Rev. B **65**, 035406 (2001).
[16] Z.-P. Liu, S. J. Jenkins, and D. A. King, J. Am. Chem. Soc. **126**, 10746 (2004).
[17] SCALAPACK: http://www.netlib.org/scalapack/scalapack_home.html
[18] In the SIESTA [J. M. Soler *et al.*, J. Phys.: Condens. Matter **14**, 2745 (2002)] calculations, Troullier-Martins norm-conserving scalar relativistic pseudopotentials were used. The energy cutoff for the real space grid used to represent the density was 100 Ry. The localization radii of the basis functions were determined from an energy-shift of 0.020 eV. The gradient-corrected exchange and correlation functional [J. P. Perdew, K. Burke, and M. Ernzerhof, Phys. Rev. Lett. **77**, 3865 (1996)], referred to as GGA-PBE, was used. The accuracy of the SIESTA method has been benchmarked with the plane-wave code previously (see Ref. 11).